CHEMISTRY OF MATERIALS

ARTICLE

pubs.acs.org/cm

Earth Abundant Element $Cu_2Zn(Sn_{1-x}Ge_x)S_4$ Nanocrystals for Tunable Band Gap Solar Cells: 6.8% Efficient Device Fabrication

Grayson M. Ford,[†] Qijie Guo,[†] Rakesh Agrawal,*[,†] and Hugh W. Hillhouse*[,†,‡]

[†]Chemical Engineering, Purdue University, West Lafayette, Indiana 47907, United States

Supporting Information

ABSTRACT: $Cu_2Zn(Sn_{1-x}Ge_x)S_4$ nanocrystals have been synthesized via batch reaction in oleylamine with no additional surfactants present. The nanocrystals are knife-coated on molybdenum substrates and then selenized to form a dense layer of $Cu_2Zn(Sn_{1-x}Ge_x)(S,Se)_4$, which is then used as the photoabsorbing layer in a thin film solar cell. The band gaps of the nanocrystals and the resulting solar cells are demonstrated to be controlled by adjusting the Ge/(Ge+Sn) ratio of the nanocrystal synthesis precursors. Solar cells fabricated from Cu_2ZnGeS_4 nanocrystal films yielded a power conversion efficiency of 0.51%. However, $Cu_2Zn(Sn_xGe_{1-x})S_4$ nanocrystals with a Ge/(Ge+Sn) ratio 0.7 yielded devices with an efficiency of 6.8% when synthesized to be Cu-poor and Zn-rich. This result opens the possibility of forming Ge gradients to direct minority carriers away from high recombination interfaces and significantly improve the device efficiency of CZTSSe-based solar cells.

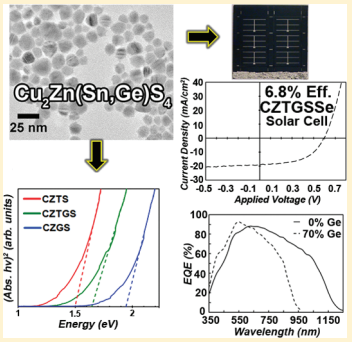

KEYWORDS: CZTS, CZTGS, CZTGSSe, CZTSSe, germanium, thin film, photovoltaic, low-cost

Earth abundant materials are a requirement for solar cells to contribute power on the multiterawatt scale.[1] $Cu_2ZnSn(S,Se)_4$ is of particular interest due to the achievement of 9.6% efficient laboratory scale devices[2] using a nonvacuum, hydrazine-based deposition process. Although hydrazine poses safety challenges from a manufacturing perspective, an alternative nonvacuum deposition approach has achieved 7.2% efficiency via the selenization of Cu_2ZnSnS_4 (CZTS) nanocrystals deposited by roll coating.[3] The resulting $Cu_2ZnSn(S,Se)_4$ (CZTSSe) film has a band gap of approximately 1.1 eV, similar to $CuInSe_2$. $CuInSe_2$ device performance is improved by incorporation of Ga,[4−6] which widens the band gap. We hypothesized that similar bandgap tuning and improvements to CZTS devices may be possible by substituting a lower atomic number group IV element for some of the Sn. Substitution with germanium is an attractive route, as germanium's crustal abudance of 1.5 mg/kg[7] (or 1.6 mg/kg[8]) compares favorably with the 2.3 mg/kg crustal abundance of Sn, the rarest element in CZTS.[7] Here we report a synthesis of $Cu_2Zn(Sn_{1-x}Ge_x)S_4$ (CZTGS) nanocrystals and the performance of $Cu_2Zn(Sn_{1-x}Ge_x)(S_ySe_{1-y})_4$ (CZTGSSe) solar cells fabricated by sintering the nanocrystal films with elemental selenium vapor. We find that the band gap of the CZTGS nanocrystals and the CZTGSSe solar cell can be rationally controlled by adjusting the Ge/(Sn+Ge) ratio.

There have been previous reports of band gap control in $(ZnS)_x(Cu_2SnS_3)_{1-x}$ nanocrystals.[9,10] However, such structures do not preserve the kesterite cation ordering observed in CZTS (or CZTGS) which appears to be critical to obtain good photovoltaic performance. CZTS nanocrystal syntheses previously reported[11−13] involve the combination of metal salt precursors and sulfur in the presence of oleylamine, and the CZTGS synthesis procedure reported here is similar.[14] The previous CZTS syntheses involved sulfur addition anywhere between room temperature and 300 °C. In contrast, we find the temperature at which sulfur is added plays a critical role in achieving the desired crystal structure and stoichiometry.[15,16]

Powder X-ray Diffraction (PXRD, Figure 1) shows the prominent peaks observed in the synthesized nanocrystals correspond with those of tetragonal CZTS (JCPDS no. 26−0575) and CZGS (JCPDS no. 25−0327). CZTS has been reported to have two related tetragonal crystal stuctures, known as stannite ($I\bar{4}2m$) and kesterite ($I\bar{4}$).[17] It is interesting to note that the stannite phase has the same symmetry as a specific disordering of the kesterite phase; the $I\bar{4}2m$ symmetry is the result of a relatively low-energy Cu−Zn cation exchange occurring randomly in the kesterite phase.[18] Although the similarity in atomic numbers between Cu, Zn and Ge contribute to the difficultly in distinguishing between stannite and kesterite using PXRD,[18] peak broadening[11,13] further obscures proper identification. The tetragonal CZGS structure found in experimental studies has been typically assigned to the stannite phase,[19,20] but the values of $c/a \leq 2$ indicate the kesterite phase (possibly with cation disorder) may be a more accurate description.[18] The most intense peaks shared by the kesterite and stannite phases agree well with the most intense peaks observed in Figure 1, indicating the nanocrystals have a tetragonal crystal structure. A shoulder observed to the left of the (112) peak could be caused by a Cu_2S impurity phase,[21] stacking faults related to cation disordering similar to the faulting in $CuInSe_2$,[22] or an orthorhombic CZGS impurity phase.[23−25] CZTGS nanocrystals were synthesized by replacing $GeCl_4$ in the CZGS synthesis with an equivalent molar

Received: January 27, 2011
Revised: March 23, 2011
Published: April 28, 2011

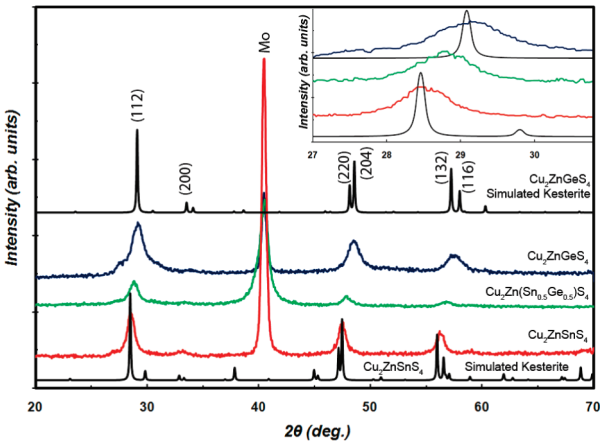

Figure 1. PXRD of $Cu_2Zn(Sn_{1-x}Ge_x)S_4$ nanocrystals for $x = 0$ (red), 0.5 (green), and 1.0 (blue). Also included for comparison are the simulated PXRD patterns for the kesterite structures of CZTS and CZGS.

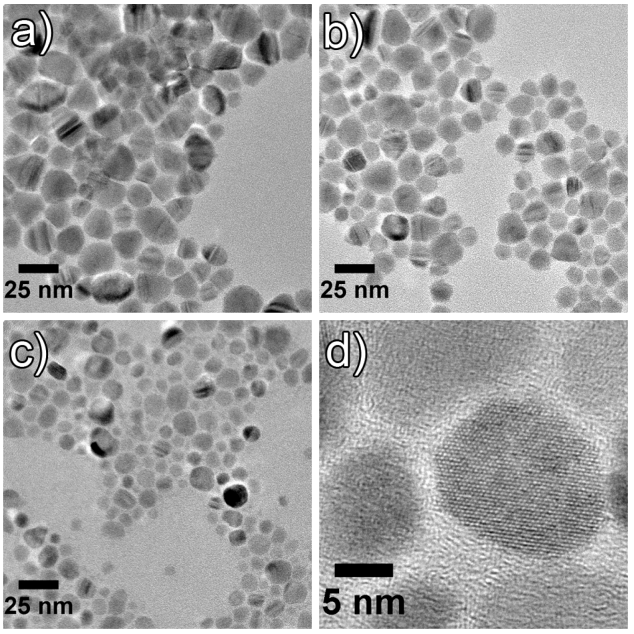

Figure 2. TEM images of (a) CZTS, (b) CZTGS, and (c) CZGS. (d) HR-TEM of CZGS nanocrystals.

amount of $Sn(acac)_2Cl_2$.[26] The expected (112) peak shift due to Sn incorporation (increasing the lattice constants) is observed by PXRD and shown in the inset of Figure 1.

The TEM images in Figure 2 reveal that the CZTGS nanocrystals vary in size from 5 to 30 nm, with the relative number of smaller sized particles increasing with increasing Ge content. The composition of the synthesized CZTGS nanocrystals as determined by energy-dispersive X-ray spectroscopy (EDS) is shown in Figure 3, with the observed elemental ratios normalized to equal 1.0 for stoichiometric CZTGS. The molecular formulas were determined to be $Cu_2Zn_{0.92}Sn_{1.11}S_{4.37}$, $Cu_2Zn_{0.97}(Sn_{0.69}Ge_{0.31})_{1.12}S_{4.73}$, $Cu_2Zn_{1.02}(Sn_{0.41}Ge_{0.59})_{1.10}S_{4.68}$, and $Cu_2Zn_{1.09}Ge_{1.03}S_{4.80}$ for nanocrystals synthesized with Ge/(Sn+Ge) precursor ratios of 0.0, 0.3, 0.5, and 1.0, respectively. The cation ratios of the nanocrystals are close to the expected stoichiometry, but there is an apparent excess of sulfur. This could be due to

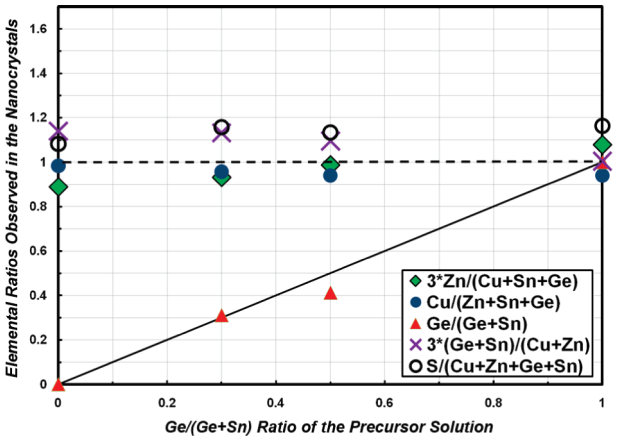

Figure 3. Various atomic ratios determined by energy-dispersive spectroscopy (EDS) showing the nanocrystals are close to stoichiometric. See text for molecular formulas.

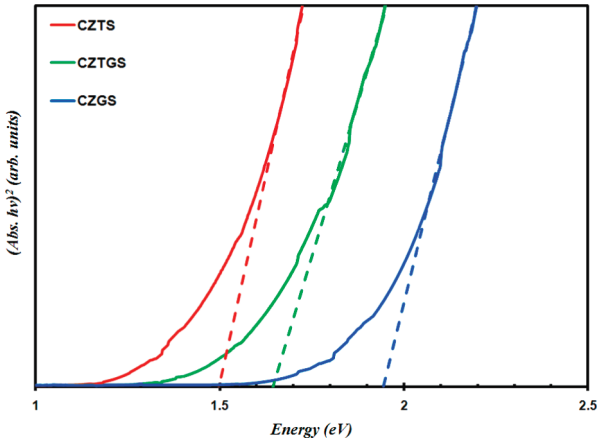

Figure 4. UV−vis data depicting the increasing onset of absorption with increasing Ge content in CZTS (red), CZTGS (green), and CZGS (blue).

matrix effects of the nanocrystal film, the lower EDS accuracy for lighter elements (i.e., sulfur) or organosulfur compounds formed during nanocrystal synthesis.

Figure 4 depicts UV−vis data for CZTGS nanocrystals with Ge/(Sn+Ge) ratios of 0.0, 0.5, and 1.0. The absorption is not expected to be influenced by quantum confinement effects, as the majority of the nanocrystals (with average diameters of 15.4, 13.3, and 8.6 nm (N = 35) for CZTS, CZTGS and CZGS, respectively) are much larger than the Bohr exciton radius of bulk CZTS, estimated to be 2.6 nm using the values reported by Persson.[27] The band gap is observed to increase with increasing Ge content of the synthesis precursors. The expected band gap for CZTS is ~1.5 eV, whereas the band gap for CZGS has been reported to be 2.05−2.25 eV.[28,29] Linear extrapolation of the nanocrystal light absorption versus the photon energy is typically used to determine the effective band gap. As shown in Figure 4, if the CZTS data are extrapolated to yield a bandgap of 1.5 eV, then the CZGS nanocrystals would have a band gap of 1.94 eV. Note that this band gap is slightly lower than those previously reported for bulk CZGS and may be due to the inherent error in the extrapolation. However, this value is distinctly different from the band gaps of Cu_2GeS_3 (0.5 eV[30]), ZnS (>3.4 eV), or GeS_2

dx.doi.org/10.1021/cm2002836 |Chem. Mater. 2011, 23, 2626–2629

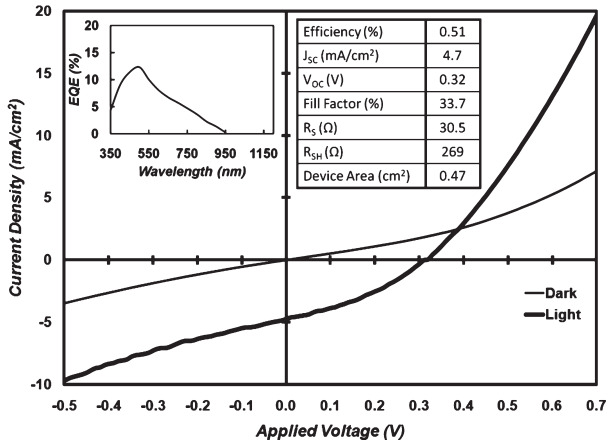

Figure 5. Current−voltage behavior of champion CZGSSe solar cell in dark and under simulated AM1.5G. Inset: EQE.

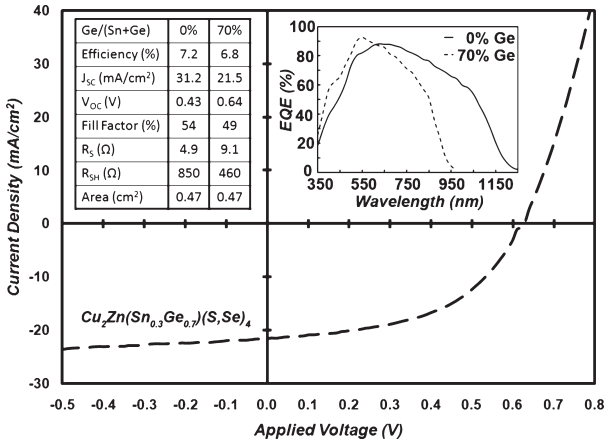

Figure 6. Current−voltage behavior of champion CZTGSSe solar cell under AM1.5G simulated illumination using a Ge/(Ge+Sn) ratio of 0.70. Inset: comparison of EQE for CZTSSe[3] and CZTGSSe devices.

(3.4 eV[31]), and is consistent with Ge being incorporated into the CZTS crystal structure.

To determine the suitability of the nanocrystals for solar cells, we fabricated CZGS nanocrystal films into devices using methods explained in detail elsewhere.[3,32,33] Briefly, the nanocrystals were thoroughly washed, and a paste of the nanocrystal ink was formed by adding hexanethiol to the dried nanocrystals to yield a formulation with ∼200 mg of nanocrystals per mL of solution. The paste was then coated onto a Mo-coated soda-lime glass (SLG) substrate with a doctor-blading technique before being annealed under Se atmosphere at 500 °C for 20 min. After annealing, standard device fabrication steps were employed to obtain devices with a SLG/Mo/CZGSSe/CdS/*i*-ZnO/ITO/Ni−Al architecture and an area of 0.47 cm^2. The current−voltage behavior (Figure 5) under AM1.5G simulated illumination revealed a total area efficiency of 0.51%. The External Quantum Efficiency (EQE, Figure 5 inset) is observed to reach 0% at 950 nm, indicating the band gap is at most no larger than 1.3 eV. This agrees well with one reported CZGSe band gap of 1.29 eV,[34] but is lower than another report of 1.52 eV.[35] Modeling of CZGSe[18] reveals the band gap can vary from 1.21−1.50 eV, with lower band gaps being indicative of lower quality (higher disorder). This also indicates that comparisons of band gaps in the CZTGSSe material system should be made between devices with similar minority carrier lifetimes and mobilities (or at minimum similar quantum efficiency curves, EQE(λ)). Additionally, a relative loss of Ge was observed during annealing under Se atmosphere.[36] Another reason for the low efficiency is the use of relatively stoichiometric nanocrystals (stoichiometric cation ratios). Typical high efficiency devices in this material class are Cu-poor and Zn-rich,[2,3,37] and our previous work with CZTS nanocrystals has shown that composition control can lead to significant improvements in device performance.[3,11]

We find that this is also the case in the CZTGS system. Although composition is still being optimized for devices, significant improvements can be obtained with high-Ge content CZTGS nanocrystals synthesized using an alternate procedure found to result in a similar Cu-poor and Zn-rich composition.[11,38] CZTGS nanocrystals synthesized with Ge/(Ge+Sn), Cu/(Zn+Sn+Ge) and Zn/(Sn+Ge) ratios of 0.70, 0.80, and 1.20, respectively, were fabricated into solar cells using the same methods described above. Champion total area device efficiency was found to be 6.8%, with the current−voltage behavior depicted in Figure 6. Band gaps determined from the EQE[39] (Figure 6 inset) of the CZTGSSe device and a similarly made CZTSSe device[3] are 1.40 and 1.11 eV, respectively. Note that the same technique to determine band gap cannot be applied to the EQE of the CZGSSe device since the decay in the EQE is most likely dominated by low minority carrier lifetime and mobilities, not the functional form of the absorption coefficient. The S/(S+Se) ratio in the devices were similar and were determined to be 0.54, 0.54, and 0.50 for the CZTSSe, CZTGSSe and CZGSSe devices, respectively (note that this analysis overestimates S content due to the presence of the CdS layer and the overlap of the S Kα and Mo Lα X-ray emission peaks). As a result, variation in band gap is not attributed to selenium content. The data presented here demonstrate Ge incorporation can be used for band gap control of both CZTGS nanocrystals and the resulting solar cells, while retaining promising device efficiency.

In summary, semiconductor nanocrystals were synthesized using Cu, Zn, Sn and Ge salts and were concluded to span the CZTGS tetragonal system based on PXRD, TEM, EDS, and UV−vis absorption. Tin-free CZGS nanocrystals fabricated into devices using a low cost roll coating approach had an efficiency of 0.51%. Device efficiency was improved to 6.8% using Ge/(Ge+Sn) = 0.70 CZTGS nanocrystals with Cu-poor and Zn-rich stoichiometry synthesized by an alternate method. This important result establishes the prospect of significant device efficiency improvements by adjusting or layering the Ge content (similar to Ga gradients in CIGSe).

■ ASSOCIATED CONTENT

Supporting Information. Experimental details, nanocrystal composition at different sulfur injection temperatures, and supporting PXRD and EDX data (PDF). This material is available free of charge via the Internet at http://pubs.acs.org.

■ AUTHOR INFORMATION

Corresponding Author

*E-mail: agrawalr@purdue.edu (R.A.); h2@uw.edu (H.W.H.).

Present Addresses

‡Chemical Engineering, University of Washington, Seattle, WA 98195, United States.

■ ACKNOWLEDGMENT

We are thankful for financial support from the NSF IGERT program (award number 0903670-DGE). We also acknowledge Samantha Hahn for her assistance in performing nanocrystal syntheses.

■ REFERENCES

(1) Wadia, C.; Alivisatos, A. P.; Kammen, D. M. *Environ. Sci. Technol.* **2009**, *43*, 2072.
(2) Todorov, T. K.; Reuter, K. B.; Mitzi, D. B. *Adv. Mater.* **2010**, *22*, E156.
(3) Guo, Q.; Ford, G. M.; Yang, W.; Walker, B.; Agrawal, R.; Hillhouse, H. W. *J. Am. Chem. Soc.* **2010**, *132*, 17384–17386.
(4) It is interesting to note that the optimum Ga concentration for $Cu(In,Ga)Se_2$ solar cells coincides with a minimization of tetragonal distortion ($c/a = 2$).[5,6] The tetragonal distortion of $Cu_2Zn(Sn,Ge)(S,Se)_4$ for kesterite is $c/a < 2$, whereas for stannite, $c/a > 2$.[14]
(5) Abou-Ras, D.; Caballero, R.; Kaufmann, C; Nichterwitz, M; Sakurai, K.; Schorr, S.; Unold, T.; Schock, H. W. *Phys. Status Solidi* **2008**, *2*, 135.
(6) Hanna, G.; Jasenek, A.; Rau, U.; Schock, H. W. *Thin Solid Films* **2001**, *387*, 71.
(7) In *CRC Handbook of Chemistry and Physics*, 91st ed. (Internet version); Haynes, W. M., Ed.; CRC Press/Taylor and Francis, Boca Raton, FL, 2011.
(8) Holl, M.; Kling, M.; Schroll, E. *Ore Geol. Rev.* **2007**, *30*, 145–180.
(9) Dai, P.; Shen, X.; Lin, Z.; Feng, Z.; Xu, H.; Zhan, J. *Chem. Commun.* **2010**, *46*, 5749–5751.
(10) Liu, Q.; Zhao, Z.; Lin, Y.; Guo, P.; Li, S.; Pan, D.; Ji, X. *Chem. Commun.* **2011**, *47*, 964–966.
(11) Guo, Q.; Hillhouse, H. W.; Agrawal, R. *J. Am. Chem. Soc.* **2009**, *131*, 11672.
(12) Riha, S. C.; Parkinson, B. A.; Prieto, A. L. *J. Am. Chem. Soc.* **2009**, *131*, 12054.
(13) Steinhagen, C.; Panthani, M. G.; Akhavan, V.; Goodfellow, B.; Koo, B.; Korgel, B. A. *J. Am. Chem. Soc.* **2009**, *131*, 12554.
(14) In a typical Cu_2ZnGeS_4 synthesis, 1 mmol of $Cu(acac)_2$, 0.5 mmol of $Zn(acac)_2 \cdot xH_20$, 0.5 mmol of $GeCl_4$, and 15 mL of oleylamine are added to a reaction vessel using standard air-free techniques. While increasing the temperature to 280 °C, 2 mmol of sulfur is added at 160 °C. The reaction is held at 280 °C for 1 h before cooling, washing, and collecting the product. See the Supporting Information for further detail on the synthesis procedure.
(15) Sulfur injections at 130 or 225 °C result in Zn deficient CZGS nanocrystals, even when up to 20% excess Zn is used (see Figures S1 and S2 in the Supporting Information).
(16) The injections at 225 °C result in nanocrystals with an upredicted (112) peak location (see the Supporting Information, Figure S5).
(17) Nakamura, S.; Maeda, T.; Wada, T. *Jpn. J. Appl. Phys.* **2010**, *49*, 121203.
(18) Chen, S.; Gong, X. G.; Walsh, A.; Wei, S. *Phys. Rev. B* **2009**, *79*, 165211.
(19) Parasyuk, O. V.; Piskach, L. V.; Romanyuk, Y. E.; Olekseyuk, I. D.; Zaremba, V. I.; Pekhnyo, V. I. *J. Alloys Cmpd.* **2005**, *397*, 85.
(20) Moodie, A. F.; Whitfield, H. J. *Acta Crystallogr., Sect. B* **1986**, *42*, 236–247.
(21) See the Supporting Information, Figure S4, for a comparison of the expected PXRD peak positions of various impurity phases in the CZGS system.
(22) Guo, Q.; Kim, S. J.; Kar, M.; Shafarman, W. N.; Birkmire, R. W.; Stach, E. A.; Agrawal, R.; Hillhouse, H. W. *Nano Lett.* **2008**, *8*, 2982–2987.
(23) Doverspike, K.; Dwight, K.; Wold, A. *Chem. Mater.* **1990**, *2*, 194.
(24) Chen, S.; Walsh, A.; Luo, Y.; Yang, J.; Gong, X. G.; Wei, S. *Phys. Rev. B* **2010**, *82*, 195203.
(25) This synthesis could form ZnS and Cu_2GeS_3 instead of CZGS; the peak at 29.06° 2θ that is assigned to the CZGS (112) could result from the sum of ZnS and Cu_2GeS_3, which have peaks centered at 28.56 and 29.26° 2θ. However, this would disagree with the UV−vis data in Figure 4.
(26) See Experimental Details section of the Supporting Information.
(27) Persson, C. *J. Appl. Phys.* **2010**, *107*, 053710.
(28) Leon, M.; Levcenko, S.; Serna, R.; Gurieva, G.; Nateprov, A.; Merino, J. M.; Friedrich, E. J.; Fillat, U.; Schorr, S.; Arushanov, E. *J. Appl. Phys.* **2010**, *108*, 093502.
(29) Matsushita, H.; Ichikawa, T.; Katsui, A. *J. Mater. Sci.* **2005**, *40*, 2003.
(30) Collaboration: Authors and editors of the volumes I.II/17H-17I-41E: Cu2GeS3 crystal structure, lattice parameters, physical properties. *SpringerMaterials—The Landolt−Börnstein Database*; Madelung, O., Rössler, U., Schulz, M., Eds.; Springer: New York; http://www.springermaterials.com, DOI: 10.1007/10717201_135.
(31) Nikolic, P. M.; Popovic, Z. V. *J. Phys. C: Solid State Phys.* **1979**, *12*, 1151.
(32) Guo, Q.; Hillhouse, H. W.; Agrawal, R. *J. Am. Chem. Soc.* **2009**, *131*, 11672.
(33) Guo, Q.; Ford, G. M.; Hillhouse, H. W.; Agrawal, R. *Nano Lett.* **2009**, *9*, 3060.
(34) Schleich, D. M.; Wold, A. *Mater. Res. Bull.* **1977**, *12*, 111.
(35) Lee, C.; Kim, C. *J. Korean Phys. Soc.* **2009**, *37*, 364.
(36) See the Supporting Information, Figure S7 and S8.
(37) Katagiri, H.; Jimbo, K.; Yamada, S.; Kamimura, T.; Maw, W.; Fukano, T.; Ito, T.; Motohiro, T. *Appl. Phys. Express* **2008**, *1*, 041201.
(38) Altered CZTGS nanocrystal synthesis procedure details discussed in the Supporting Information, Figures S2 and S5.
(39) Zoppi, G.; Forbes, I.; Miles, R. W.; Dale, P. J.; Scragg, J. J.; Peter, L. M. *Prog. Photovoltaics: Res. Appl.* **2008**, *17*, 315–319.